ChemComm

COMMUNICATION

View Article Online
View Journal | View Issue

Cite this: *Chem. Commun.*, 2021, **57**, 13558

Received 31st August 2021,
Accepted 21st November 2021

DOI: 10.1039/d1cc04847c

rsc.li/chemcomm

Self-crystallisation, an unexpected property of 45S5 Bioglass®†

Djurdja Vukajlovic, Katarina Novakovic and Oana Bretcanu *

Self-crystallisation of 45S5 Bioglass® powder and scaffolds was observed one year after their fabrication. Plate- and acicular-shape crystals, identified as calcium and sodium carbonates, grew at room temperature and atmospheric pressure, without any further treatment.

Bioactive glasses are well known for their osteointegration properties. When immersed in physiological solutions, they degrade and release ions which facilitate the precipitation of hydroxyapatite on their surface. This hydroxyapatite is similar to the inorganic component of natural bone, accelerating the bone growth on its surface. Thus, when implanted in bone tissue, bioactive glasses will degrade in favour of newly formed bone tissue.[1]

The first and most studied bioactive glass was developed by Hench in the 1970s.[2] It has a composition of 45% SiO_2, 24.5% Na_2O, 24.5% CaO and 6% P_2O_5 (wt%) and has been commercialised under the name 45S5 Bioglass®. Since then, different compositions of bioactive glasses have been developed for applications in bone tissue engineering, such as bone defect fillers, 3D porous scaffolds, medical device coatings and bone cement composites.[3] Many studies have been focused on scaffold preparation which requires a heat treatment during which bioactive glasses crystallise, forming glass-ceramics with enhanced mechanical properties. However, these glass-ceramics are less reactive than the parent glasses, as ions contained in the glass network (such as Na^+, Ca^{2+} and Si^{4+}) are entrapped in the crystalline phases, decreasing the dissolution rate. During sintering, 45S5 Bioglass® has a high tendency to undergo crystallisation. The main crystalline phases were identified as $Na_2Ca_2Si_3O_9$ and $Na_2CaSi_2O_6$. Secondary crystalline phases such as $Na_2Ca_4(PO_4)_2SiO_4$ have also been reported.[4,5]

School of Engineering, Newcastle University, Newcastle upon Tyne, NE1 7RU, UK. E-mail: oana.bretcanu@ncl.ac.uk

† Electronic supplementary information (ESI) available: Detailed experimental procedures; supplementary data. See DOI: 10.1039/d1cc04847c

Herein, we report self-crystallisation of 45S5 Bioglass® powders and glass-ceramic scaffolds at room temperature and atmospheric pressure without any further heat treatment. To our knowledge, this is the first report of self-crystallisation of 45S5 Bioglass® powders and scaffolds, observed after one year in storage. As with many discoveries, chance played an important role in identifying this phenomenon. In 2020, due to the Covid pandemic, our laboratories were closed. One year later we revisited our samples and we observed some of the stored samples on a scanning electron microscope (SEM). To our surprise, plate-shape and acicular crystals (less than 15 μm in size), had grown on the surface of 45S5 Bioglass® samples. Hence, an investigation into the type of these crystals, their structure and possible mechanism of crystallisation has been conducted. It is worth noting that this phenomenon has been observed only on 45S5 Bioglass® samples. We analysed another silicate bioactive glass, apatite–wollastonite (see details in ESI†), but we did not observe any crystals grown on the surface of apatite–wollastonite glass powder or glass-ceramic scaffolds.

The 45S5 Bioglass® powders and glass-ceramic scaffolds were kept in sealed plastic bags in the laboratory, at room temperature, and were analysed one year after their fabrication. The SEM images and X-ray diffraction (XRD) spectra were compared with the ones taken pre-storage (a few days after their fabrication).

Fig. 1 shows SEM images of 45S5 Bioglass® powders one year after their fabrication. Plate- and blade-shape crystals grew from the glass surface, having their long axis as a preferential growth direction. Plates are 5–8 μm in length, 2–5 μm wide and less than 0.5 μm thick (Fig. 1A). Over time, plates split, forming blade-shape crystals, less than 2 μm wide (Fig. 1B). Crystal splitting likely occurs due to crystal growth.

Thin layers of flat crystals with lamellar structure can be noticed in Fig. 1C and Fig. S1 (ESI†). These lamellar plates have a preferred orientation, with nearby crystals being roughly parallel. It seems that these lamellar plates undergo crystallisation from the surface of the glass. The plates grow and split into slabs or columns (Fig. 1D) and bladed crystals (Fig. 1B).

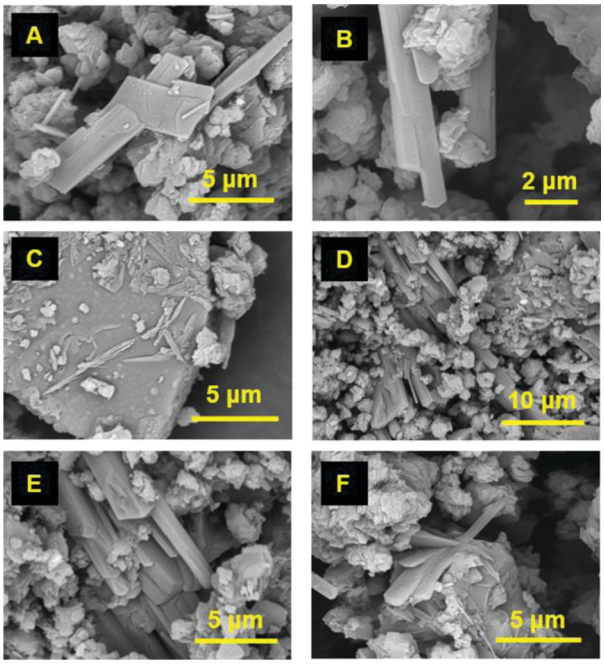

Fig. 1 SEM images of 45S5 Bioglass® powder after one year in storage (all images were taken in 2021).

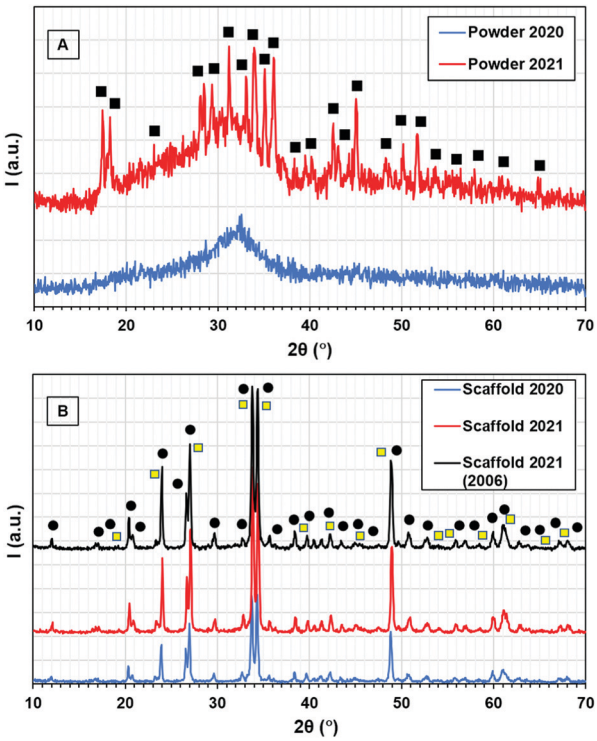

Fig. 2 XRD patterns of 45S5 Bioglass® powders (A) and scaffolds (B) a few days after their preparation (2020) and after storage for one year (2021); scaffold 2021 (2006) was fabricated in 2006 and analysed in 2021, after 15 years in storage (■ = $Na_2Ca(CO_3)_2{\cdot}2H_2O$, ● = $Na_2Ca_2Si_3O_9$, □ = Na_2CO_3).

Single columns can contain parallel blade-shape crystals that split over time (Fig. 1E). Columnar crystals taper to an edge or have a blunt termination (Fig. 1E). Some blade-shape crystals form fan-shape clusters, as seen in Fig. 1F (radiating cluster of crystals).

The diffraction patterns of the 45S5 Bioglass® powder taken a few days after preparation (2020) and one year later (2021) are presented in Fig. 2A. After glass preparation, XRD data show an amorphous structure. A characteristic amorphous halo can be observed in the range $2\theta = 15–40^\circ$. One year later, crystallisation peaks identified as sodium calcium carbonate hydrate, $Na_2Ca(CO_3)_2{\cdot}2H_2O$, were observed on the glass surface. $Na_2Ca(CO_3)_2{\cdot}2H_2O$ has an orthorhombic structure (plate- and column-shape crystals), in agreement with SEM data. The average crystallite size was 58 ± 9 nm.

Formation of carbonates is not unusual. In geology, natural silicate rocks and minerals react with atmospheric CO_2 forming insoluble carbonates (over a geological time scale) and SiO_2. Industrial processes such as mineral carbonation or mineral sequestration use natural olivine, serpentine, wollastonite, *etc.* (calcium, magnesium and iron silicates) to capture CO_2 for storage.[6,7]

As mentioned above, the 45S5 Bioglass® powders were kept at room temperature in a sealed bag in the lab. Typically, the temperature and relative humidity in the lab vary between 14–20 °C and 50–80%, respectively, depending on the weather. These conditions bear no resemblance to industrial processes or geological time frames. It may be postulated that the 45S5 Bioglass® powder reacted with the CO_2 and water vapours present in the bag, forming hydrated sodium and calcium carbonates. The crystals grew to a maximum dimension of 10 μm, probably due to limited availability of CO_2 and water vapours in the sealed bag.

Several studies reported that bioactive glasses with high alkaline content in their composition are typically hygroscopic.[8–11] The presence of hydroxyl ions on the surface of the bioglass powders promotes their crystallisation,[8] in agreement with our results.

Fig. 3A and Fig. S2 (ESI†) show SEM images of the 45S5 Bioglass® scaffolds one year after their fabrication. Bunches of needle-like crystals can be observed on the surface of the scaffolds. These acicular crystals are about 10–15 μm in length and they seem to grow intergranularly, along their long crystallographic axis (Fig. 3B). The V-shape of the bundles suggests a simple splitting mechanism where a single crystal nucleates from a single nucleus, grows to a certain 'critical' length and then splits into smaller size crystals that are not separated from each other at the base (nucleation point).

It is worth noting that similar clusters of acicular crystals were reported by Mondal *et al.*[12] for a sol–gel derived bioactive glass with a composition of $70SiO_2$, 26CaO and $4P_2O_5$ (mol%), after a hydrothermal process (36 h at 170 °C) (Fig. S3, ESI†). Those acicular crystals had a size of 2–10 μm and were identified as hydroxyapatite.

Fig. 3C and D show SEM images of 45S5 Bioglass® scaffolds one year apart, a few days after synthesis (2020) and one year later (2021), respectively. No needle-like crystals are observed on the surface of the scaffold (Fig. 3C) a few days after its

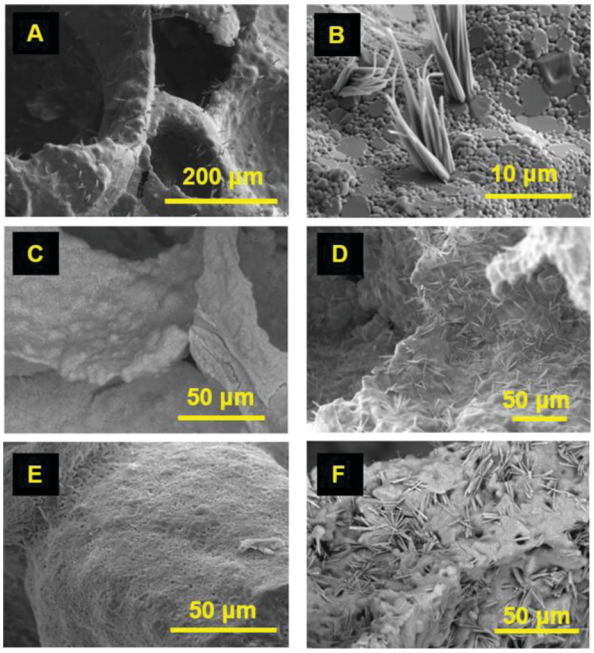

Fig. 3 SEM images of 45S5 Bioglass® glass-ceramic scaffolds (images A, B and D were taken in 2021, after one year in storage; images C and E were taken in 2020 and 2006, respectively, a few days after scaffolds preparation; image F was taken in 2021, after 15 years in storage).

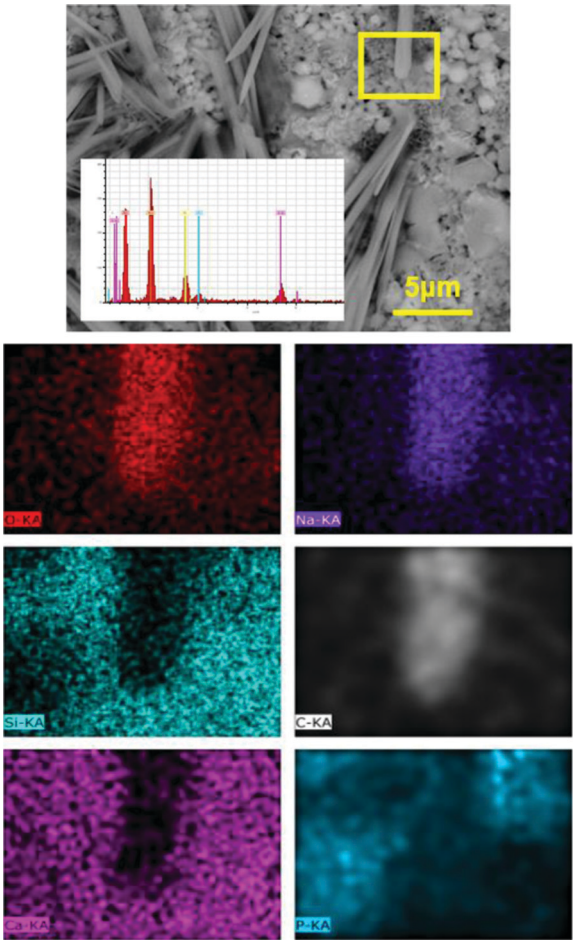

Fig. 4 EDS map analysis of the marked region (yellow rectangle) on the surface of 45S5 Bioglass® glass-ceramic scaffold after one year in storage (image taken in 2021).

fabrication. However, one year after scaffolds fabrication, clusters of acicular crystals, maximum 15 μm in length, are detected (Fig. 3D). Similar results were obtained with older 45S5 Bioglass® scaffolds made in 2006 (Fig. 3E and F). Recent (2021) SEM images of a 45S5 Bioglass® scaffold synthesised in 2006 indicate clusters of acicular crystals (Fig. 3F). Surprisingly, the length of these crystals is maximum 15 μm, similar to the one-year-old scaffolds, despite being 15 years old.

The energy dispersive spectroscopy (EDS) map analysis of an acicular crystal (Fig. 4) indicates that these needles are mainly composed of Na, O and C. The atomic ratio of O/C and O/Na likely correspond to a sodium carbonate structure. Several authors reported calcium or sodium carbonate formation on the surface of bioglasses[13–15] when both CO_2 and water vapours are present.

XRD spectra of the 45S5 Bioglass® scaffolds taken a few days after synthesis (2020) and after one year in storage (2021) are presented in Fig. 2B. The XRD pattern of a 45S5 Bioglass® glass-ceramic scaffold made in 2006 and re-examined in 2021 is also included (Fig. 2B). The main crystalline phase was identified as $Na_2Ca_2Si_3O_9$. The average crystallite size was 50 ± 8 nm. Acicular crystals were identified as Na_2CO_3, which are soluble in water. This was demonstrated by immersing the scaffolds in distilled water for 15 min. SEM analysis showed that the acicular crystals were completely dissolved (see Fig. S4, ESI†).

The growth of these acicular crystals might involve diffusion of carbon in a solid state, which has very slow kinetics. Carbon diffusion probably starts at grain boundaries, rich in Na^+ ions. Smaller size Na^+ ions have higher mobility than Ca^{2+} ions and accumulate at the surface. Nucleation probably starts at the grain boundaries, where there is more space for the nuclei to form, consuming Na^+ ions. The regions around the growing crystals have lower Na^+ concentration so another crystal cannot grow nearby in a Na-depleted region. This explains the non-homogeneous distribution of the acicular crystals on the surface of the scaffold which favours the growth of vertically oriented crystals.

In conclusion, 45S5 Bioglass® powder and scaffolds can undergo self-crystallisation at room temperature and atmospheric pressure without any further processing. SEM analysis indicates initial formation of plate-shape crystals on the surface of 45S5 Bioglass® powder, which subsequently split into blade- and column-shape crystals. The plate crystals were identified as hydrated sodium and calcium carbonates. Considering the glass-ceramic scaffolds, acicular crystals of sodium carbonate were observed on their surface.

This short communication provides some valuable information on the unique self-crystallization mechanisms of 45S5 Bioglass®, but there are still more questions to be answered. Why does the glass powder aid the formation of plate-like crystals while the glass-ceramic promotes acicular structure?

This might be related to glass and glass-ceramic reactivity, specific surface area and local variations of chemical composition. Are there other bioglasses that may undergo self-crystallisation? Are other types of crystals likely to grow with different bioglass formulations or storage conditions? Further investigation needs to be carried out to understand this phenomenon. Studying early stages of the self-crystallisation of 45S5 Bioglass® powder and glass-ceramic will provide more insights on the crystallisation mechanisms and factors that can accelerate or inhibit nucleation and crystallisation. Formation of these plate- and acicular-shape crystals leads to a temporary increase in specific surface area which could be beneficial for several applications such as accelerated osteointegration or enhanced drug delivery.

Djurdja Vukajlovic: investigation, formal analysis, validation, funding acquisition; Katarina Novakovic: conceptualisation, writing – review & editing, funding acquisition; Oana Bretcanu: conceptualisation, investigation, formal analysis, writing – original draft.

This work was supported by Newcastle University Overseas Research Scholarship (NUORS) Award and School of Chemical Engineering and Advanced Materials International Postgraduate Scholarship (CEAMIPS) funding.

Conflicts of interest

There are no conflicts of interest to declare.

Notes and references

1 L. L. Hench, Bioceramics, *J. Am. Ceram. Soc.*, 1998, **81**(7), 1705–1728, DOI: 10.1111/j.1151-2916.1998.tb02540.x.
2 L. L. Hench, The story of Bioglass®, *J. Mater. Sci.: Mater. Med.*, 2006, **17**(11), 967–978, DOI: 10.1007/s10856-006-0432-z.
3 L. L. Hench, Opening paper 2015 - Some comments on Bioglass: Four eras of discovery and development, *Biomed. Glasses*, 2015, **1**, 1–11, DOI: 10.1515/bglass-2015-0001.
4 L. Lefebvre, L. Gremillard, J. Chevalier, R. Zenati and D. Bernache-Assolant, Sintering behaviour of 45S5 bioactive glass, *Acta Biomater.*, 2008, **4**(6), 1894–1903, DOI: 10.1016/j.actbio.2008.05.019.
5 O. Bretcanu, X. Chatzistavrou, K. Paraskevopoulos, R. Conradt, I. Thompson and A. R. Boccaccini, Sintering and crystallisation of 45S5 Bioglass® powder, *J. Eur. Ceram. Soc.*, 2009, **29**(16), 3299–3306, DOI: 10.1016/j.jeurceramsoc.2009.06.035.
6 A. A. Olajire, A review of mineral carbonation technology in sequestration of CO_2, *J. Pet. Sci. Eng.*, 2013, **109**, 364–392, DOI: 10.1016/j.petrol.2013.03.013.
7 R. Chang, S. Kim, S. Lee, S. Choi, M. Kim and Y. Park, Calcium Carbonate Precipitation for CO_2 Storage and Utilization: A Review of the Carbonate Crystallization and Polymorphism, *Front. Energy Res.*, 2017, **5**, 17, DOI: 10.3389/fenrg.2017.00017.
8 S. Lopez-Estebana, E. Saiz, S. Fujino, T. Oku, K. Suganuma and A. P. Tomsia, Bioactive glass coatings for orthopedic metallic implants, *J. Eur. Ceram. Soc.*, 2003, **23**(15), 2921–2930, DOI: 10.1016/S0955-2219(03)00303-0.
9 S. Fujino, H. Tokunaga, E. Saiz and A. P. Tomsia, Fabrication and Characterization of Bioactive Glass Coatings on Co–Cr Implant Alloys, *Mater. Trans.*, 2004, **45**(4), 1147–1151, DOI: 10.2320/matertrans.45.1147.
10 H. R. Fernandes, A. Gaddam, A. Rebelo, D. Brazete, G. E. Stan and J. M. F. Ferreira, Bioactive Glasses and Glass-Ceramics for Healthcare Applications in Bone Regeneration and Tissue Engineering, *Materials*, 2018, **11**(12), 2530, DOI: 10.3390/ma11122530.
11 R. Sergi, D. Bellucci and V. Cannillo, A Comprehensive Review of Bioactive Glass Coatings: State of the Art, Challenges and Future Perspectives, *Coatings*, 2020, **10**(8), 757, DOI: 10.3390/coatings10080757.
12 D. Mondal, A. Zaharia, K. Mequanint and A. S. Rizkalla, Sol-Gel Derived Tertiary Bioactive Glass-Ceramic Nanorods Prepared via Hydrothermal Process and Their Composites with Poly(Vinylpyrrolidone-Co-Vinylsilane), *J. Funct. Biomater.*, 2020, **11**(2), 35, DOI: 10.3390/jfb11020035.
13 M. Cerruti and C. Morterra, Carbonate Formation on Bioactive Glasses, *Langmuir*, 2004, **20**(15), 6382–6388, DOI: 10.1021/la049723c.
14 A. Perardi, M. Cerruti and C. Morterra, Carbonate formation on sol-gel bioactive glass 58S and on Bioglass® 45S5, *Stud. Surf. Sci. Catal.*, 2005, **155**, 461–469, DOI: 10.1016/S0167-2991(05)80173-9.
15 C. Charbonneau, F. Vanier and L. P. Lefebvre, Stability of bioactive bone graft substitutes exposed to different aging and sterilization conditions, *Int. J. Ceram. Eng. Sci.*, 2020, **2**(4), 152–161, DOI: 10.1002/ces2.10047.